Relation of stage activities
Lorenzo Blanco

Working on project:

Observation and Parameterization of Oceanic Convection (PLUME)

14/03/2024-13/08/2024

University ROMA TRE referent:

Professor Claudia Adduce

LEGI laboratory referent:

Researcher Maria Eletta Negretti

Researcher Joel Sommeria

Contents

Introduction

The stage focused on the PLUME research project in his initial stages; my work has focused mostly on the study of the temperature measurements in the experiments. Part of the work done has contributed to my master thesis focusing on studying the general phenomenon of shear-induced mixing and confronting some results obtained to the state of the art.

The oceans have a fundamental role in the CO_2 segregation and heat absorption from the atmosphere; all this happening through the mixed layer on the surface, also thanks to convective plumes generated by boundary conditions; currently these phenomena remain inadequately modelled (Huang et al.2014, Koenigk et al. 2021).

The mixed layer consists of the superficial layer of the oceans, in contact with the atmospheric winds and the nocturnal cooling; these phenomena create turbulent and convective motion which can transport heat and CO_2 at greater depths, blocking their interaction with the atmosphere for years or centuries.

Currently the convective plumes model available ignore the effects of earth rotation and are calibrated using mainly atmospheric data; this makes their application harder in more complex cases in oceans.

These problems in our models bring more uncertainty on current climate models; for this reason, a series of experiments has been done on the Coriolis Platform in Grenoble, the biggest rotating platform in the world; the objective of the experiments is to obtain enough useful data to create a new parametrization which can describe this very complex phenomena in a more accurate way.

My stage focalizes on the first and second set of experiments done from April 2024 to August 2024; the first experiments focus on the feasibility of the entire research, making sure all equipment works up to standard and verifying the consistency of the data measured with expected phenomena. The second set of experiments uses the newly constructed heating floor at the bottom of the Coriolis platform, to study both shear-induced mixing and convective plumes created by the heating.

Experimental apparatus and procedure of the experiments

The experimental apparatus consists of the Coriolis rotating platform, a 13 m diameter platform that can rotate up to 6 rotations per minute; it can be filled up to 1 meter depth.

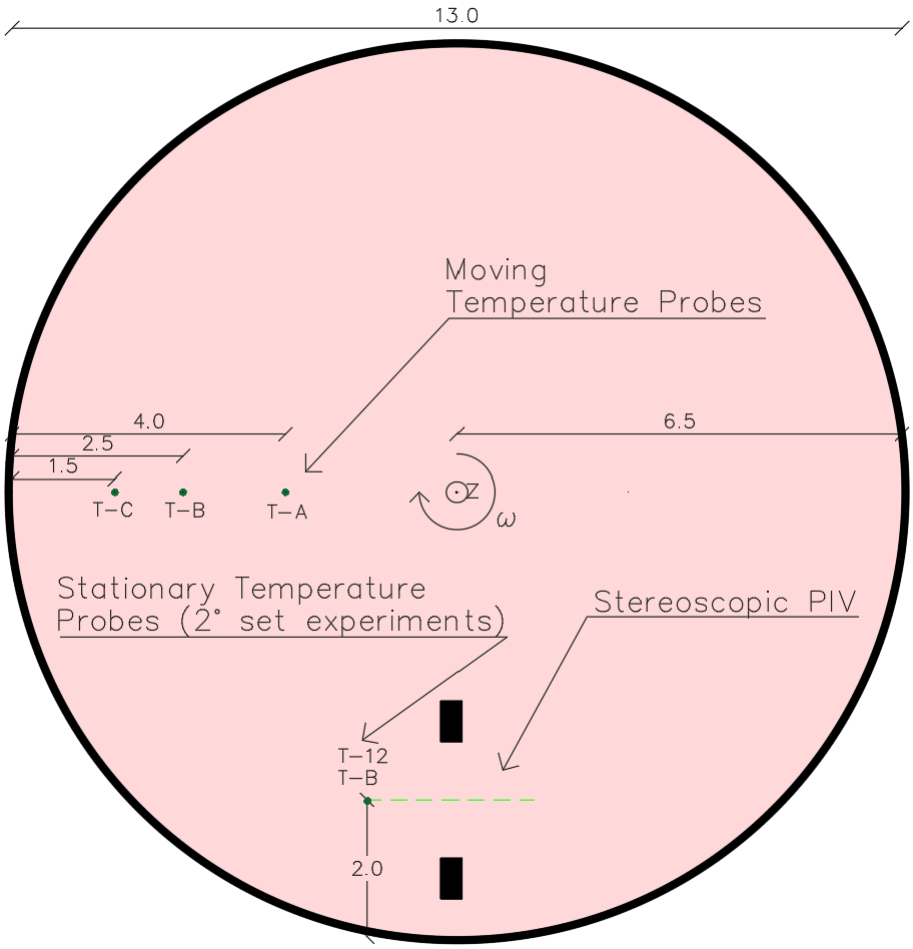

Figure 1: Experimental setup

The procedure of the first set of experiment consists in simulating the effect of wind-induced shear on the surface of the oceans using the rotation of the Coriolis platform; a procedure already used and tested by Sous et al (2013).

The water inside the tank will be either in homogeneous conditions or stratified using temperature, a few experiments have been done using salt instead.

The Coriolis platform has many inlets at the bottom to fill it; in this case, only the central inlet was used because in the second set of experiments all other inlets will be closed off; it was needed to verify that a good stratification could be obtained while filling the platform from a single inlet.

To achieve the temperature stratification inside the platform, two tanks of water have been filled out with water at ambient temperature and at a higher temperature depending on the experiment; the filling system of the platform mixes the water accordingly to guarantee that the filling starts with the hotter water and then slowly lowers the temperature by mixing the ambient temperature water as it continues to fill the platform.

The filling can take up to 3 hours or more depending on the water depth because of the use of a single inlet, during these first experiments the water depth has remained close

to constant at around only 50-51 cm; thanks to this many experiments have been made in a short amount of time.

Spin-up experiments have been made starting both from a still platform and from an already rotating platform; in the second cases the platform has been filled up while rotating to guarantee the stable stratification; the spin-up is done in such a way to guarantee the same shear at the bottom regardless of initial rotation.

The second set of experiments introduces a heating plate at the bottom of the platform, which is used to simulate the superficial cooling in oceans during the night; so, both wind-induced shear and night cooling plumes can be simulated at the same time.

Different measuring equipments were used during the first and second sets of experiments, I focused on the study of the temperature probes, so I'll be talking only about them in this relation.

Temperature probes

Three temperature probes are mounted on three vertical axes at different radiuses of the platform; they are moved up and down by motors.

Also, two other probes were positioned in the second set of experiments, one on the heating plate at the bottom and another at a height of around 12 cm from it, both not moving. These 2 probes were used to estimate the Rayleigh and the Nusselt number during experiments with no temperature stratification.

The probes work by creating and measuring an electrical current inside the water; higher temperatures lower the electric resistance of the water at the probe position, increasing the tension measured.

I've worked on the temperature probes from the start of the series of experiments, taking the raw data from them and processing it in a more accessible form to all members of the research team.

The probes require to be calibrated on water of known temperature to then interpolate a logarithmic curve which ties tension measured and temperature. A calibration was done the day before the start of the first set of experiments and this is the calibration of probe A:

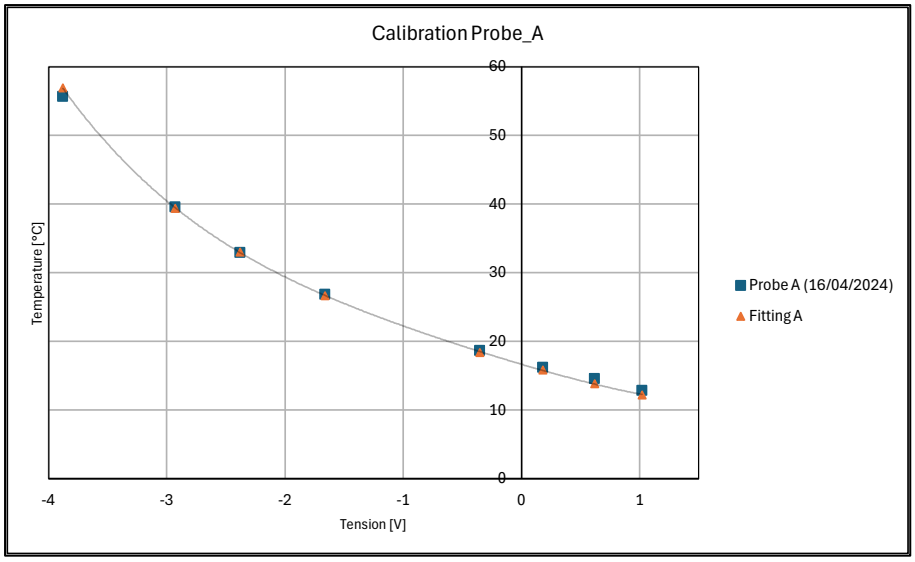

Figure 2: Calibration temperature probes

The calibration formula used for the fitting has been given by the producer of the probes:

$$V_0 = G\ exp\left(A + \frac{B}{T}\right) + V_{off} \qquad [1]$$

V_0: Tension measured by the probe [V].

T: Temperature [K].

G, A, B, V_{off}: Parameters.

By inverting the formula:

$$T = \left(\log\left(\frac{V_0 - V_{off}}{G}\right) - \frac{A}{B}\right)^{-1} \qquad [2]$$

A second calibration was done at the end of the first set of experiments to verify the parameters used; it shows very little deviation compared to the first calibration in the range of 15-30 °C which is the range of temperature of the series of experiments:

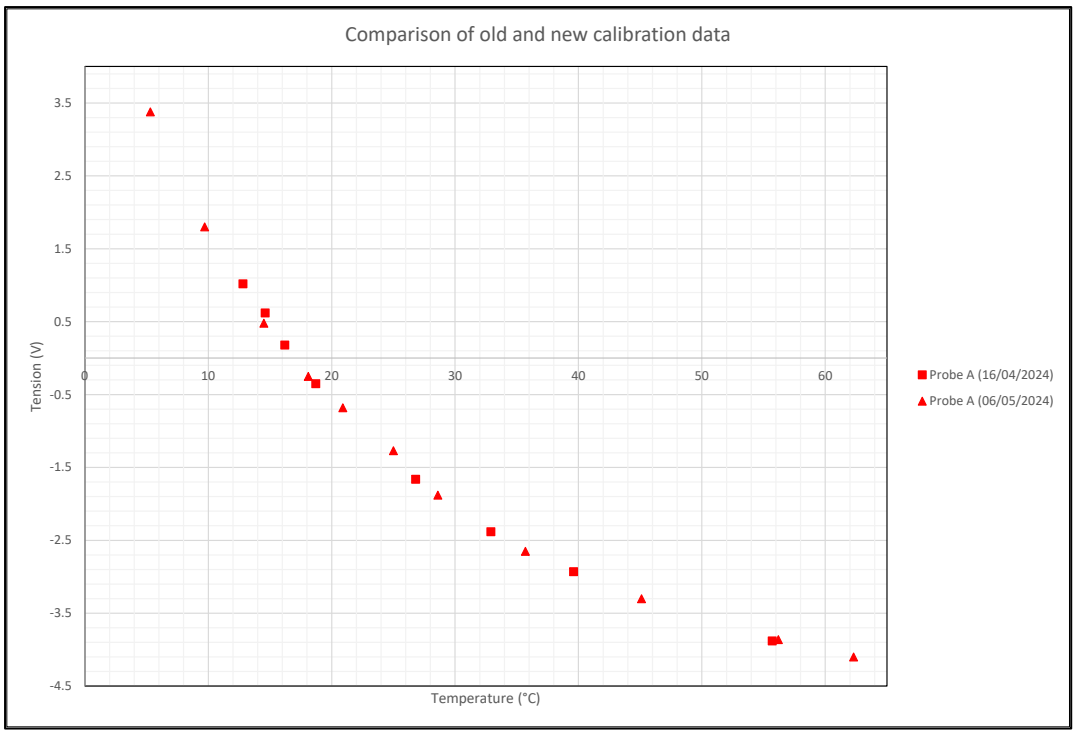

Figure 3: Comparison of two calibration made at the start and at the end of the first set of experiments

The probes can do measurements with a time frequency of 240 Hz but it's only able to measure accurately while moving towards the fluid it's measuring, so, only during the descending phase, useful data can be gathered; during the ascending phase some mixing occurs right on the probe end creating inaccurate temperature readings.

The probes move up and down to measure a profile, this means that all following profiles shown have not been measured in a single time instant but over a period varying depending on the probe speed:

Height of measurement [cm]	
50	
Probe speed [cm/s]	**Time to measure a profile [s]**
1	50
3	16.67
5	10
10	5

Table 1: Difference in time of measurement of a vertical temperature profile

Also, only the descending data can be used, so the actual time to measure a profile is higher than the value in Table 1 because the probes need to return to the top position.

The speed at which the motors move the probes has been changed over time; the phenomenon is fast developing, so it's of interest to get as many measurements as possible over the same period of time; initially the speed used was 10 cm/s but it was too fast, the reading of the probes did not correlate to an initial profile made at 1 cm/s as can be seen from these plots:

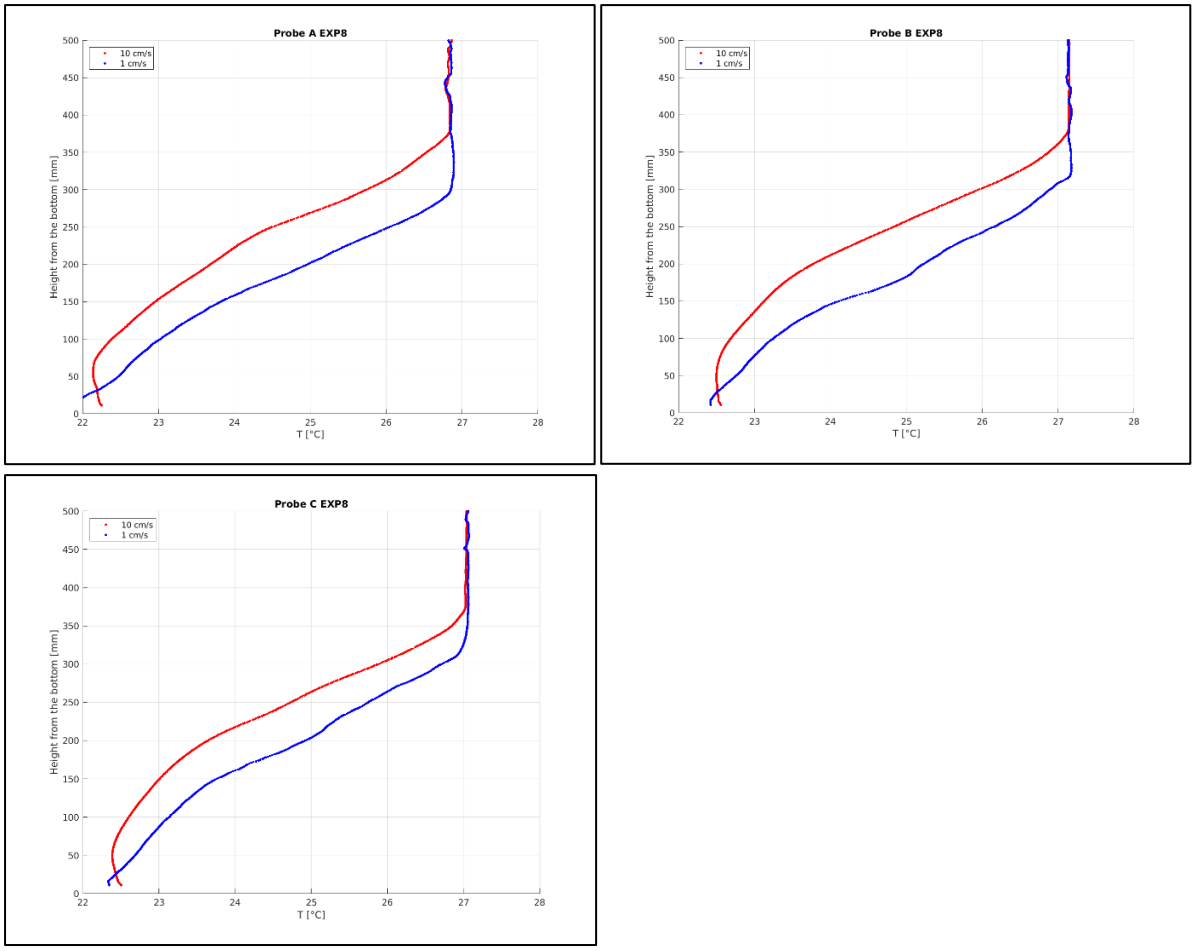

Figure 4: Difference between profiles with high and low temperature probe speed

After various tests with temperature profiles at different speed, it was chosen to maintain a speed of 3 cm/s; here is a more detailed test that was done with the platform in rotation, it's suspected that the rotation could have played a role in the measurement, but it still gives a good estimate of the difference between the different probe speeds:

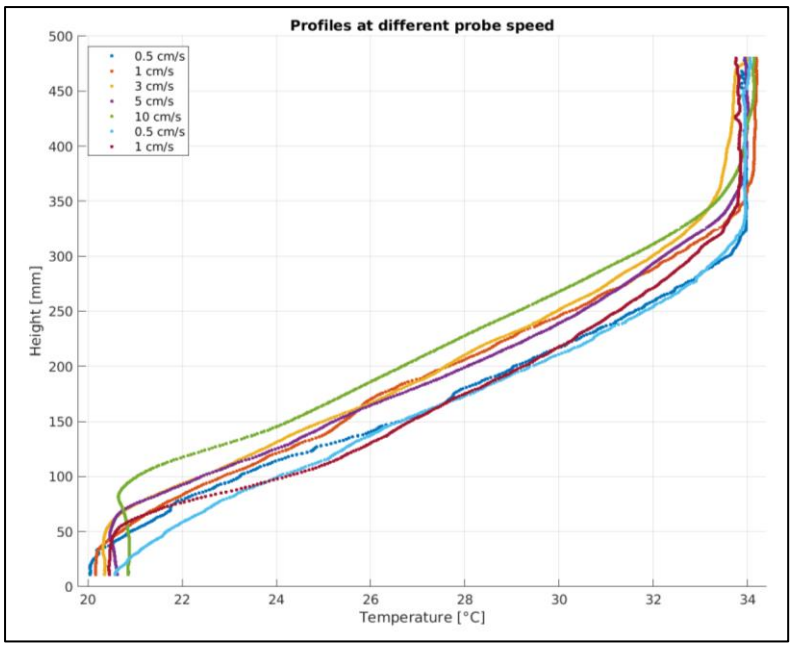

Figure 5: Comparison between different probe speeds

The discrepancy between the two reading in Figure 4 gets worse at higher speeds but doesn't get completely removed even at lower speeds. In some experiments the internal waves inside the tank can bring oscillations of the temperature profile but such discrepancy remained consistent over many experiments so it cannot be assumed to be the only reason.

Currently it's still not completely clear the reason of the big discrepancy, part of it is caused by the fact that the slow profile is done first, so it could create some mixing right on the vertical axe of the probe; at the same time, some of the errors obtained seem too high to be justified by the mixing caused by the very small probe.

Activities done

Literature studies

Before the start of the work on the data regarding the experiments, I've read in detail many scientific papers relating to the phenomena of interest; regarding both other experiments done with similarity to the research and theoretical studies regarding expected results.

The objective of the experiment is, initially, to follow the process done by H.Kato and Phillips (1969); this is one of the main reference for the first set of the experiments.

Some of the experimental results will be compared to the theoretical models developed by Pollard et all (1973) (hereafter P73) regarding the growth of the mixed layer in case of

rotation and Turner (1968) (hereafter T68) regarding the relation of the entrainment coefficient to the Richardson number.

The results of P73 show a scaling law with an initial growth of the layer as:

$$h = \frac{u_*}{\sqrt{fN}} 4(1 - cos(ft)^{\frac{1}{4}}) \qquad \text{for } t < \frac{\pi}{f} \qquad [3]$$

u_*: Friction velocity [m/s].

F: Coriolis frequency [1/s].

N: Brunt–Väisälä frequency [1/s].

t: Time [s].

P73 predicts that the growth of the mixed layer stops after one half an inertial period to:

$$h_{max} = 8^{\frac{1}{4}} \frac{u_*}{\sqrt{fN}} \qquad \text{for } t \geq \frac{\pi}{f} \qquad [4]$$

This is assuming that all parameters remain constant, but this is not always the case during the experiments as it will be shown later.

Data analysis and data plots

To study more easily the temperature data, a bidimensional matrix was created with the probe time as the columns and the height from the bottom as the rows; for each instant of time the probe data will be inserted into the correct position in the matrix, creating a diagonal filling as shown in this representation:

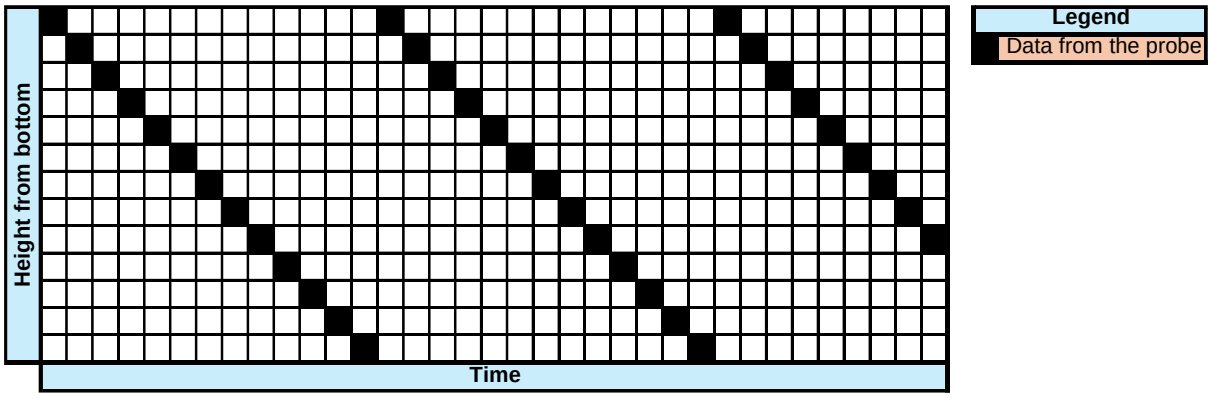

Figure 6: Data readings of the temperature probe data over time

After the data has been arranged like this, an interpolation is made for all the missing data in between; the faster the probes move, the less time passes in between the profiles so the interpolation happens over a smaller time window:

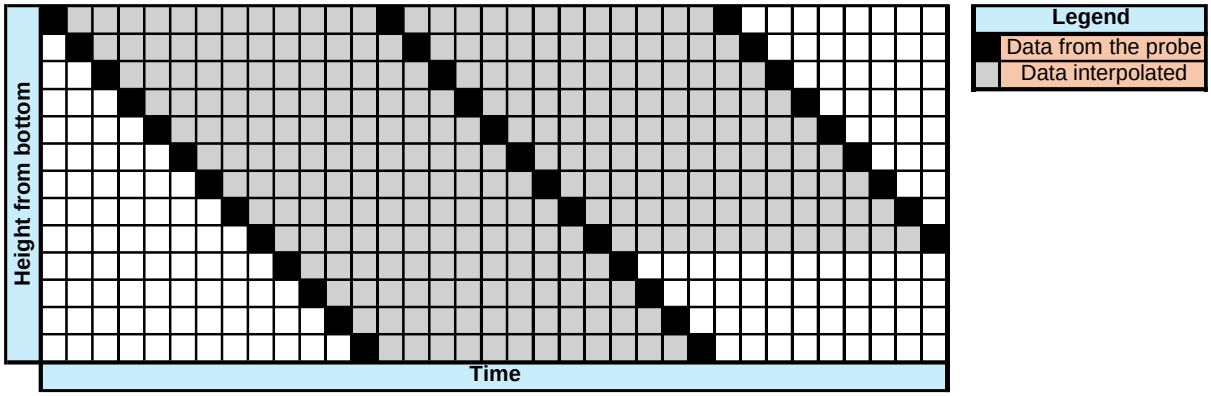

Figure 7: Interpolation of the probe data to get a time series

This makes following processing and plotting of data much easier.

1° set of experiments

Many graphical plots have been made regarding the different experiments:

- Comparison of the temperature measurements of fast- and slow-moving temperature probes:

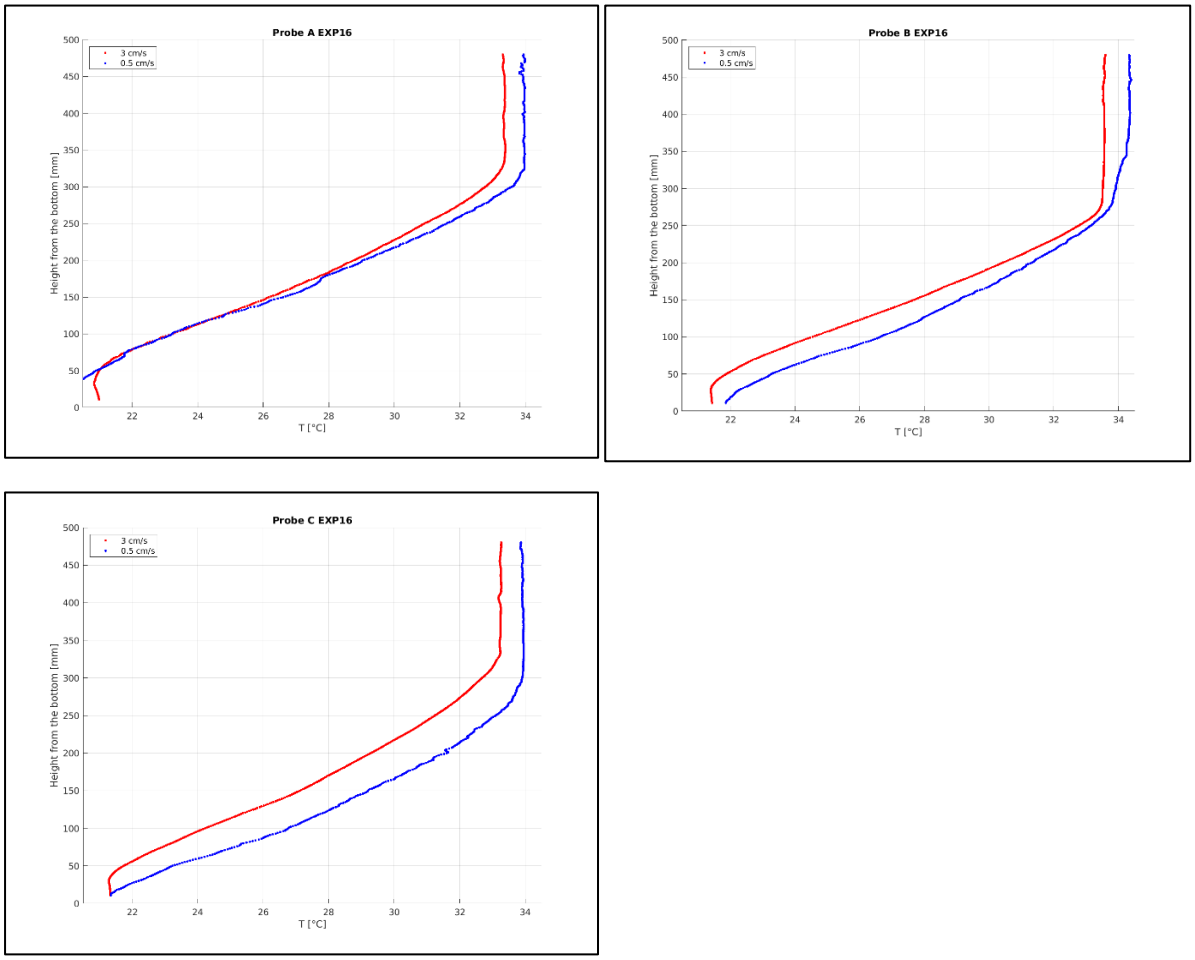

Figure 8: Comparison fast and slow-moving temperature probes measurements

These profiles have mainly been used at the start of the first set of experiments to change the velocity of the temperature probes to minimize errors.

- Animation of the change of the three temperature profiles over time (here shown 3 time instant during EXP16):

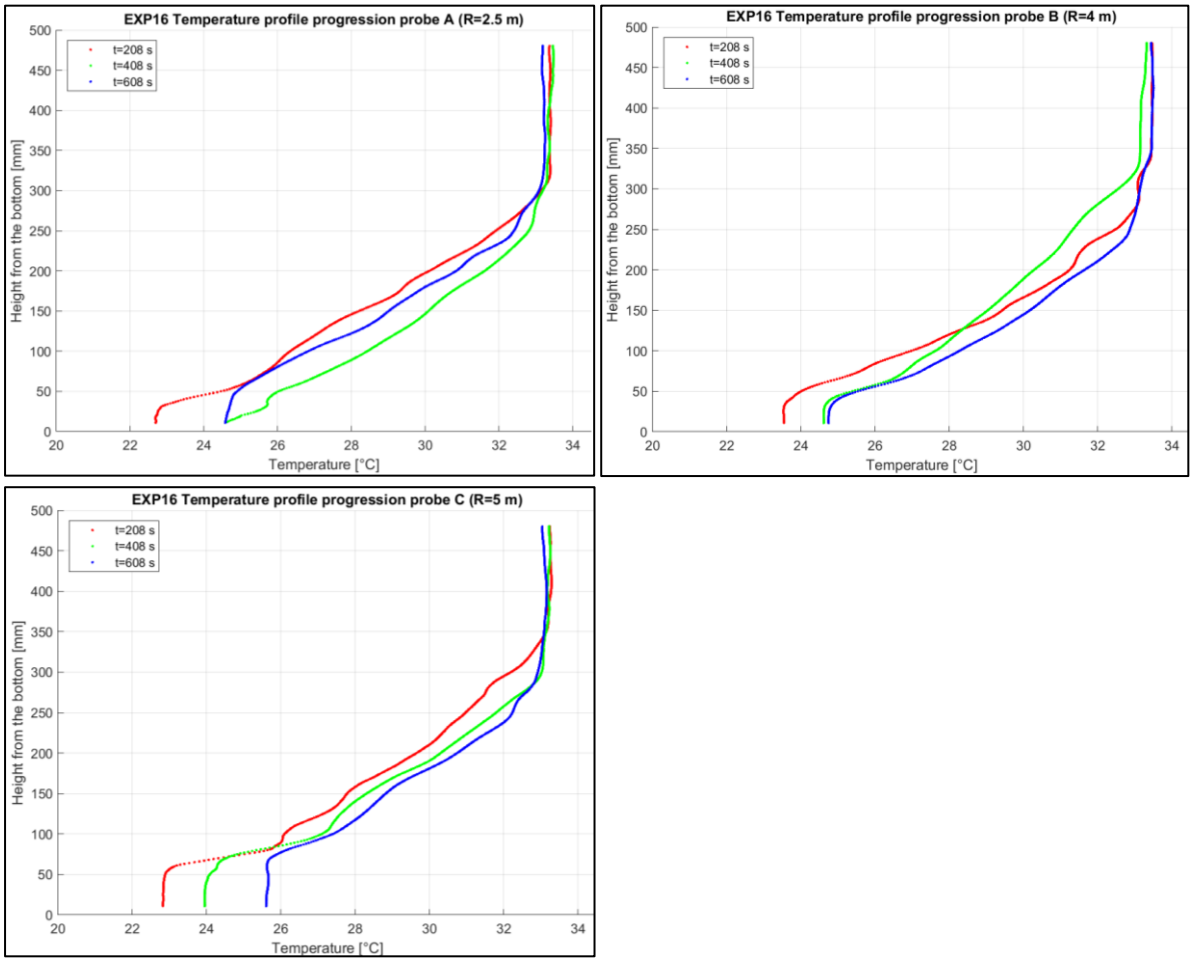

Figure 9: Progression of the temperature profile over time EXP16

These animations showed in detail the formation of the mixed layer at the bottom and showed the mixing process over time; this was very useful to visualize the mixing caused by different rotation speeds, showing a significant difference in the overall phenomenon. The animations created are the faster and most accessible way to visualize all the data gathered by the probes during the experiment.

- Temperature measurements at a fixed height over time:

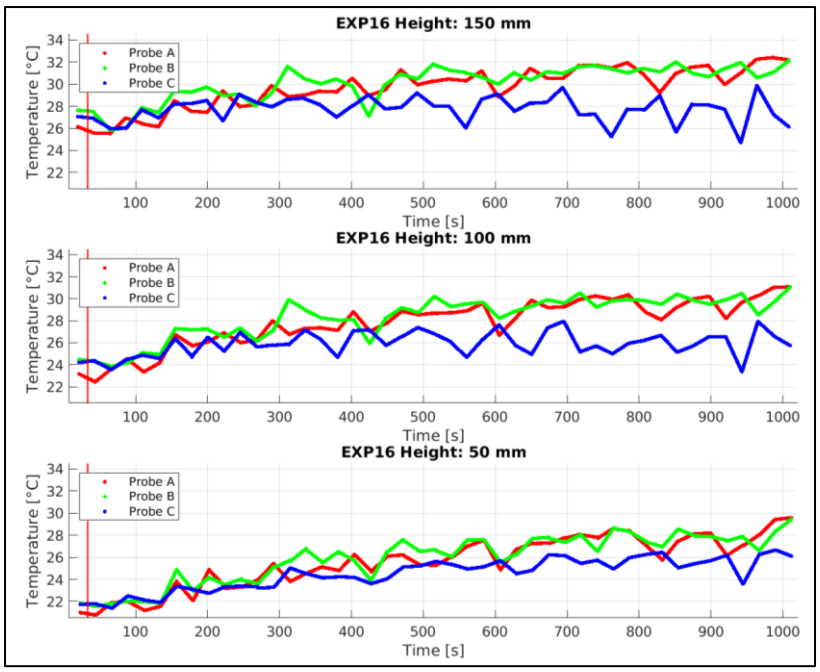

Figure 10: Temperature measurements at fixed heights over time

Useful to verify oscillations in the temperature data; they show a similarity between their period and the rotation period of the experiments, specifically the one used for the spin-up, not the initial rotation of the tank; this behaviour is consistent in most experiments.

- Estimation of the growth of the mixed layer at the bottom:

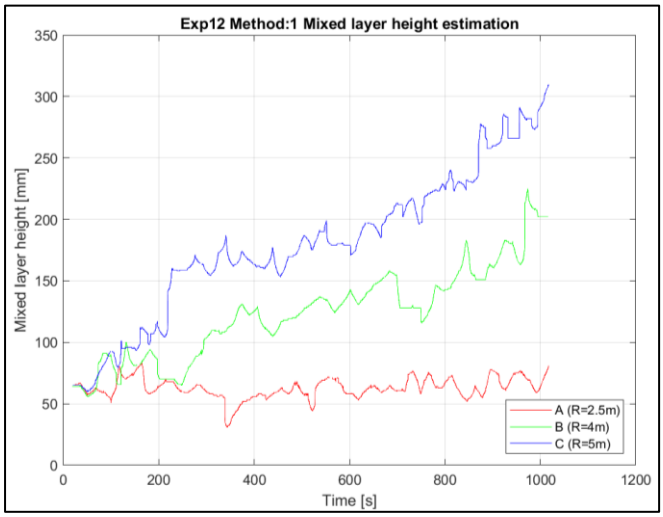

Figure 11: Mixed layer growth EXP12

The mixed layer height is significant to the phenomenon and being able to visualize its growth can help notice the differences between different rotation speed during the experiments.

The algorithm used was created by me and, after a vertical smoothing, does comparison over the derivative of the temperature profile over the vertical, using that data to estimate

the position of the mixed layer which shows a strong increase of the derivative; the algorithm was verified thanks to the temperature profile animation made.

- Comparison of the mixed layer height with P73 theoretical results:

Pollard results assume a constant N but that was not the case during the experiments, so the value is being updated over time as the stratification gets weaker, these are some of the results obtained:

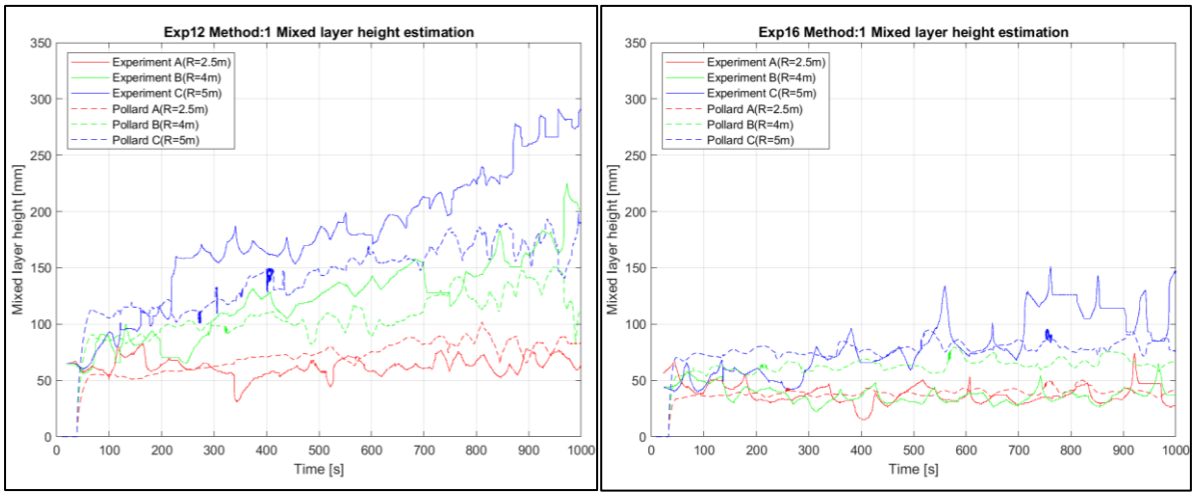

Figure 12: Mixed layer height growth compared to P73 results

The difference between experiments 12 and 16 was the period of rotation after the spin-up; EXP12 had a final rotation period of 120 seconds while EXP 16 had a final rotation period of 60 seconds.

It can be seen from the results that we are not able to capture the initial growth of the mixed layer because of the presence of a small homogeneous layer at the bottom, even before the spin-up; after that, the values predicted by P73 show a good similarity with the results obtained, the data which is further away from those results is probe C in EXP12, this can be explained by a wall boundary effect which can create a corner homogeneous region which grows over time and can falsify the results obtained.

These plots show how the higher rotation rate significantly lower the growth of the mixed layer height, even though further data analysis show how this doesn't correlate to a lowering of the mixing process in general.

- Studies of the potential energy change during the experiments

The potential energy change during the experiments shows the effect of mixing; initially I calculated the raw potential energy change over time, this shows inconsistent results:

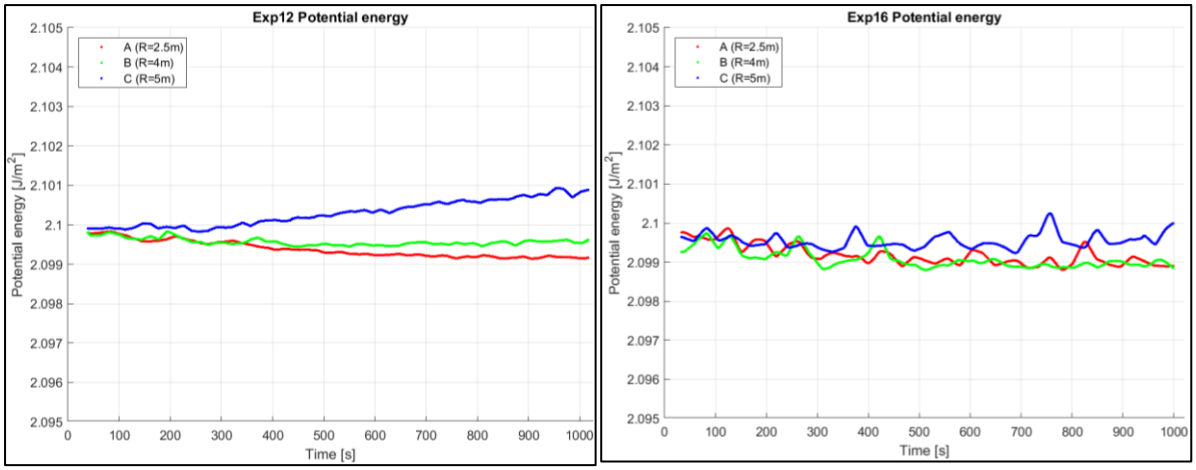

Figure 13: Raw potential energy over the vertical axes of the temperature probes

The total potential energy lowers over time, this is not consistent with the mixing process and the development of the temperature profile over time; this is caused by the radial effect; colder water at the bottom of the tank is moving towards the outer area of the tank lowering the mass closer to the centre; so, there's no mass conservation over the vertical.

To solve the problem the potential energy was divided by the total mass over time measured at the vertical axe of the temperature probe, the mass was calculated thanks to the temperature profile and the Kell equation (1975):

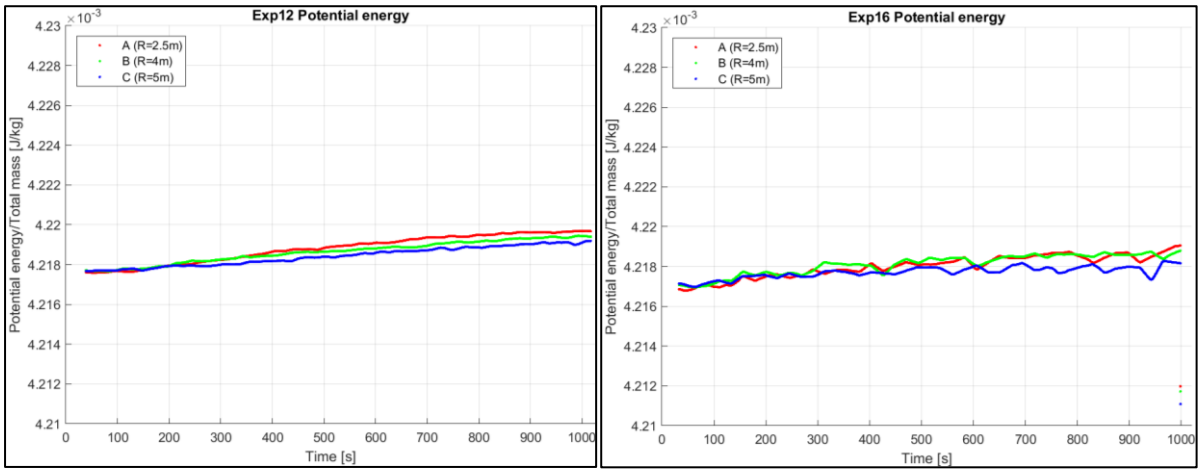

Figure 14: Potential energy divided by the total mass over time to get rid of the radial effect

The data becomes consistent with the observation from the temperature probes, now the potential energy always grows over time in all probes position.

The value has been normalized to the initial value:

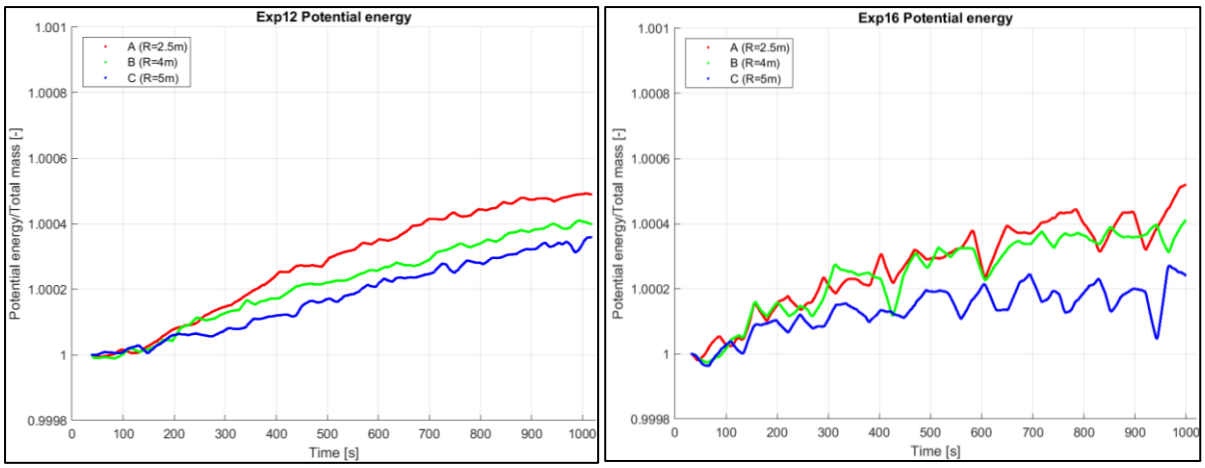

Figure 15: Potential energy over total mass normalized by the initial value

It can be seen how both experiments show an equal increase of the potential energy over time, regardless of the rotation speed before and after the spin-up. This brings the conclusion that, regardless of the growth of the mixed layer, the mixing process itself remains only dependent on the strength of the spin-up and not on initial rotation conditions.

Looking at similar data from other experiments shows a similar behaviour but do not bring such clear conclusions because of lower total experiment times (300 instead of 1000 s), much lower stratifications which reach the homogeneous conditions too early, so the potential energy stops growing earlier.

- Estimation of the radial heat flux calculated through a model that I created:

A simple model has been created to study the radial heat flux inside the platform; a radius of the platform has been divided into 4 cells divided by the three probes and with the wall and the centre of the platform as the boundaries; the loss of heat from boundary conditions has been ignored but could be very easily added:

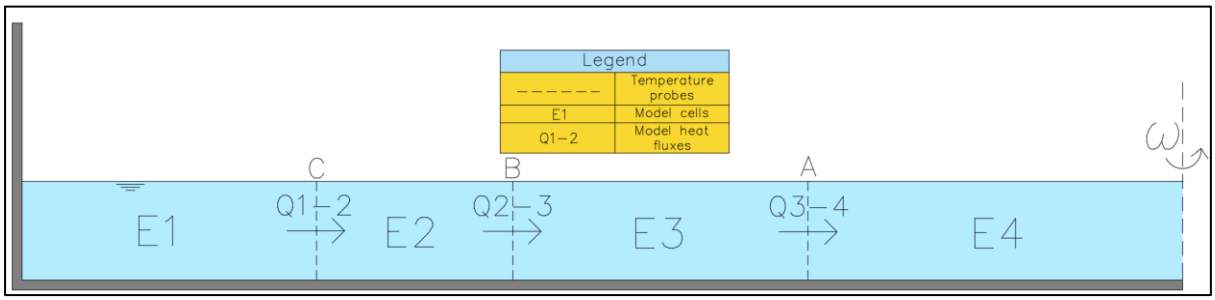

Figure 16: Model used to calculate thermal energy and thermal fluxes

In this model the only heat fluxes are the one in between the four cells and the thermal energy in each cell is only dependent on the energy of the previous time instant and the nearby fluxes. A basic system of linear equations has been created to calculate the heat fluxes by knowing some of the energy in the cells:

$$\begin{cases} E_1^{it+1} = E_1^{it} - Q_{12}^{it} * \Delta t \\ E_2^{it+1} = E_2^{it} + Q_{12}^{it} * \Delta t - Q_{23}^{it} * \Delta t \\ E_3^{it+1} = E_3^{it} + Q_{23}^{it} * \Delta t - Q_{34}^{it} * \Delta t \\ E_4^{it+1} = E_4^{it} + Q_{34}^{it} * \Delta t \end{cases} \quad [5]$$

The highlighted values are the unknown. By interpolating the temperature measurements in between the probes A, B and C, E_2 and E_3 can be estimated. The temperature of probe A has been interpolated all the way to the centre of the platform to remove the E_4 unknown, to be able to solve the system with four equations. This hypothesis is not too strong because probe A and B already show almost the same temperature between the two; close to the centre, the centrifugal force is negligeable, so the temperature is assumed constant.

The energy in cell 2,3,4 has been calculated as:

$$E_i = \sum_j T_{ij}\ \delta_{ij}\ b_i\ h_j\ C_H \quad [6]$$

T_{ij}: Temperature interpolated by the probes [K].

δ_{ij}: Density calculated from the temperature using the Kell equation (Kell 1975) [kg/m^3]

b_i: Width of the cell [m].

h_j: Height of the cell [m].

C_H: Heat capacity of water: $4186\ \left[\frac{J}{kg°C}\right]$.

i is the cell index (from 1 to 4) and j is the vertical index, necessary because of the difference in temperature over the vertical, a mean cannot be used because the Kell equation is not linear. Some of the plots obtained from this system are as follows:

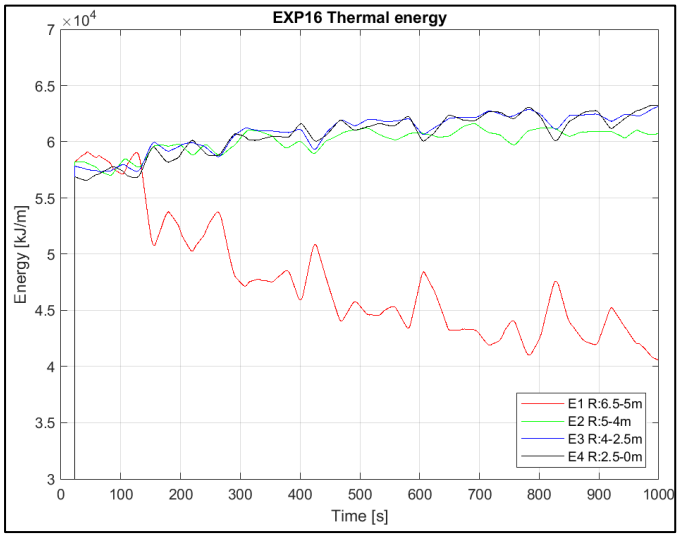

Figure 17: Thermal energy in the 4 cells of the model

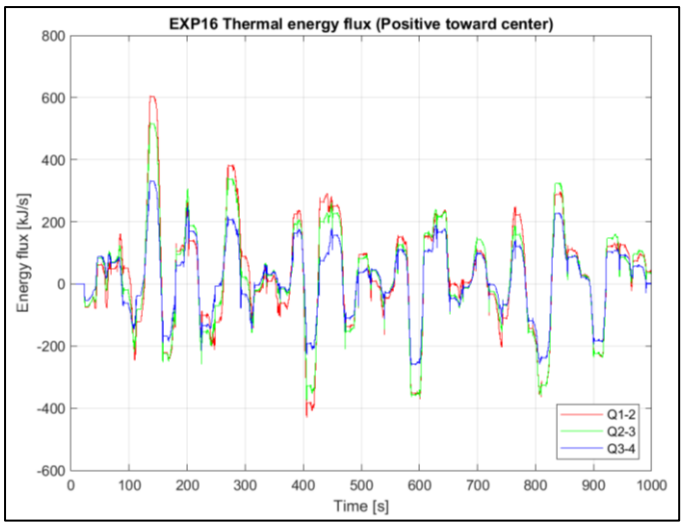

Figure 18: Thermal energy flux in between the cells

As expected, as the spin-up starts, colder water starts moving towards the outer wall of the tank, decreasing the heat energy of cell 1; while all the others increase as can be seen in Figure 17.

In Figure 18 the oscillations have a period of around 60 seconds which is the same as the period of the spin-up in EXP16, other experiments show a similar behaviour. The heat flux oscillates strongly because of the internal waves present inside the tank, but overall, it's a mean heat flux towards the centre as expected.

2° set of experiments

During the second set of experiments new temperature probes have been used; one positioned at the heating plate position, one at 12 cm of height; these can show the behaviour of the heating plate and they were used to estimate the heating plate power:

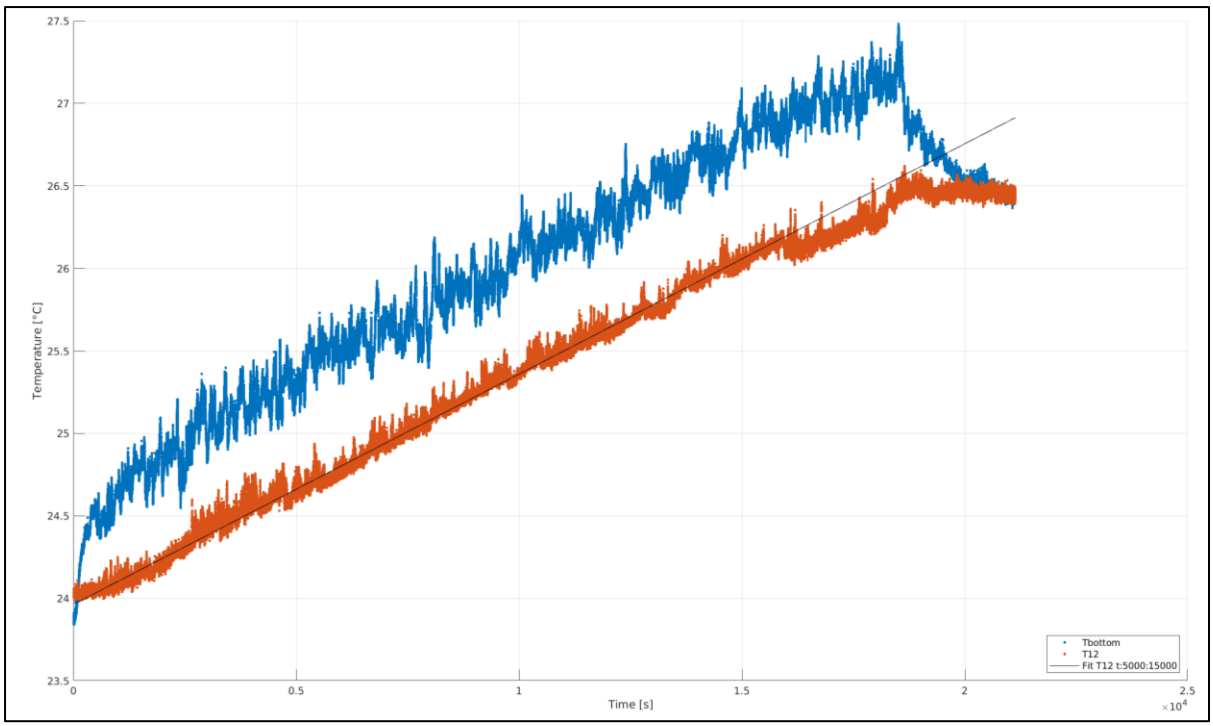

Figure 19: Temperature at on the heating plate and inside the tank over time

It can be seen the transition from the moment the plate is turned on up until it's turned off and the temperature between the two probes equalizes.

EXP22 has no temperature stratification over the vertical, the temperature remains homogeneous during the entire experiment:

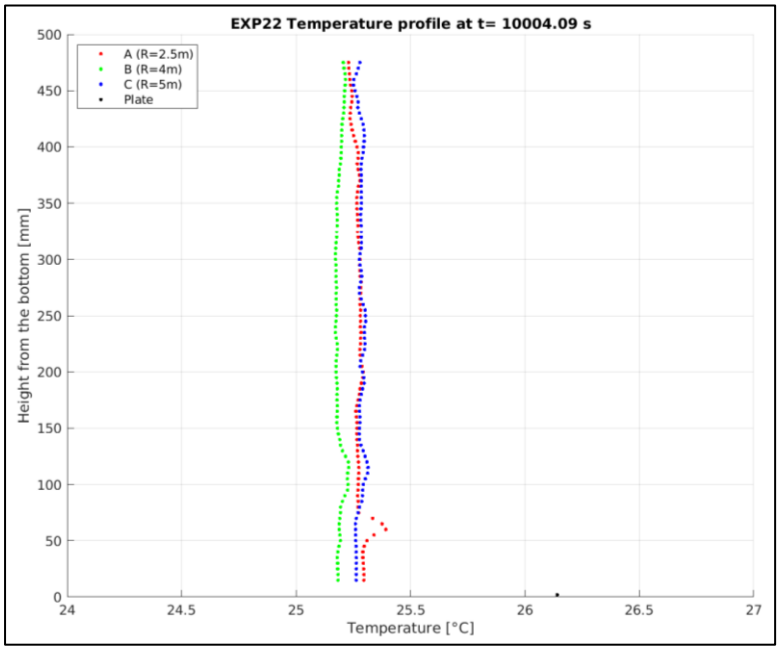

Figure 20: Example of the temperature profile during experiments with no stratification

The temperature inside the platform over time has been linearly fitted and the temperature changes over time have been used to estimate the plate energy flux.

The timeframe of interest has been from 0.5*10^4 s to 1.5*10^4 s; an average over 10^4 s which is almost 3 hours.

T12 is representative of the homogeneous temperature over the vertical.

The temperature changes from around 24.66 °C to 26.05 °C over the 10^4 s using the linear fit made in this time frame to avoid oscillations.

The total difference in thermal energy is equal to:

$$\Delta E = V\rho c_p \Delta T = A_p\, h\, \rho\, c_p (T_2 - T_1) \qquad [7]$$

V: Volume of water [m^3]

A_p: Area of the platform (assuming also the centre core is being heated as the outer area): $\pi\ 6.5^2\ m^2 = 132.73\ m^2$

h: Height of the water during the experiment: 0.5 m.

ρ: Density considered constant because of the very small change: 996.95 $\frac{kg}{m^3}$.

c_p: Heat capacity of water: 4186 $\frac{J}{kgK}$.

The change in density is negligible, going from 997.13 to 996.77 kg/m^3 according to the Kell equation (1975).

Dividing by the time gives the total power of the system:

$$P_{max} = \frac{\Delta E}{\Delta t} = \frac{A_p\, h\, \rho\, c_p}{\Delta t}(T_2 - T_1) = \frac{132.73*0.5*996.95*4186}{10\text{^}4}(26.05 - 24.66) = 38.5\ kW \quad [8]$$

The major hypothesis is that the central core of water is at the same temperature of the outer layer; in the opposite assumption that no heat enters the central core, which is also unrealistic, the area decreases to: $\pi(6.5^2 - 2.75^2) = 108.97\ m^2$ and the power decreases to 31.61 kW.

It's realistic to think that the correct heat power is somewhere in the middle of the maximum and minimum values:

$$P_{plate} = 31{,}61 \div 38.5 \quad kW \qquad [9]$$

Dividing the total power to the heat pad area, the power over the surface can be obtained:

$$A_{heat\ plate} \approx \pi(6.5^2 - 2.75^2) = 108.97\ m^2$$

$$P_{plate} = 290.08 \div 353.30\ \frac{W}{m^2} \qquad [10]$$

The minimum and maximum value change depending on the central core condition which is not known because of lack of other measurements.

The power from the heating plate has also been studied by measuring the currents passing through the power supply. There were a total of 15 cables of length 150 m, each having a current of 81.3 A; the resistance of the cables is approximately $0.244*10^{-2}$ Ω/m.

Calculating the tension in the cables:

$$V = R\,I = 0.244 * 10^{-2} * 150 * 81.3 = 29.76\,V \qquad [11]$$

Calculating the power:

$$P = V\,I * 15 = 29.76 * 81.3 * 15 = 36.3\,kW \qquad [12]$$

$$P = \frac{36.3 * 10^3}{108.97} = 333.12\,\frac{W}{m^2}$$

The value of electrical power obtained is perfectly consistent with the value obtained from the heating inside the platform verifying the previous results.

Other values estimated from the experiments

- The density stratification in the experiments has been described using the Brunt–Väisälä frequency, it consists of the frequency at which a particle of density ρ_0 subjected to an initial vertical displacement moves inside a stably stratified fluid with a stratification of $\frac{\partial \rho(z)}{\partial z}$:

$$N^2 = \frac{g}{\rho_0}\frac{\partial \rho(z)}{\partial z} \quad [s^{-2}] \qquad [13]$$

ρ_0: Reference density (set at 1000 kg/m^3).

$\frac{\partial \rho(z)}{\partial z}$: Density distribution in the experiment.

G: Gravity acceleration.

One of the objectives of the experiments is studying the relation between the entrainment coefficient and the Richardson number; it's estimated to be a dependence of the order of Ri^{-1} according to T68.

The entrainment coefficient is defined as:

$$E = \frac{u_e}{u_*} \qquad [14]$$

u_e: Entrainment speed [m/s]-

u_*: Friction velocity [m/s].

The friction velocity is going to be solely dependent on the spin-up process; all the experiments with spin-up have been done so that the friction velocity is constant in

between the experiments. The problem of calculating the entrainment speed remains, in one experiment it was possible to use to growth of the mixed layer to estimate it; the problem is that in the case of some experiments the mixing happened without a significant growth of the mixed layer, so, currently, I was only able to reproduce the KP69 approach in EXP12.

In EXP12 the results of the entrainment speed are the following:

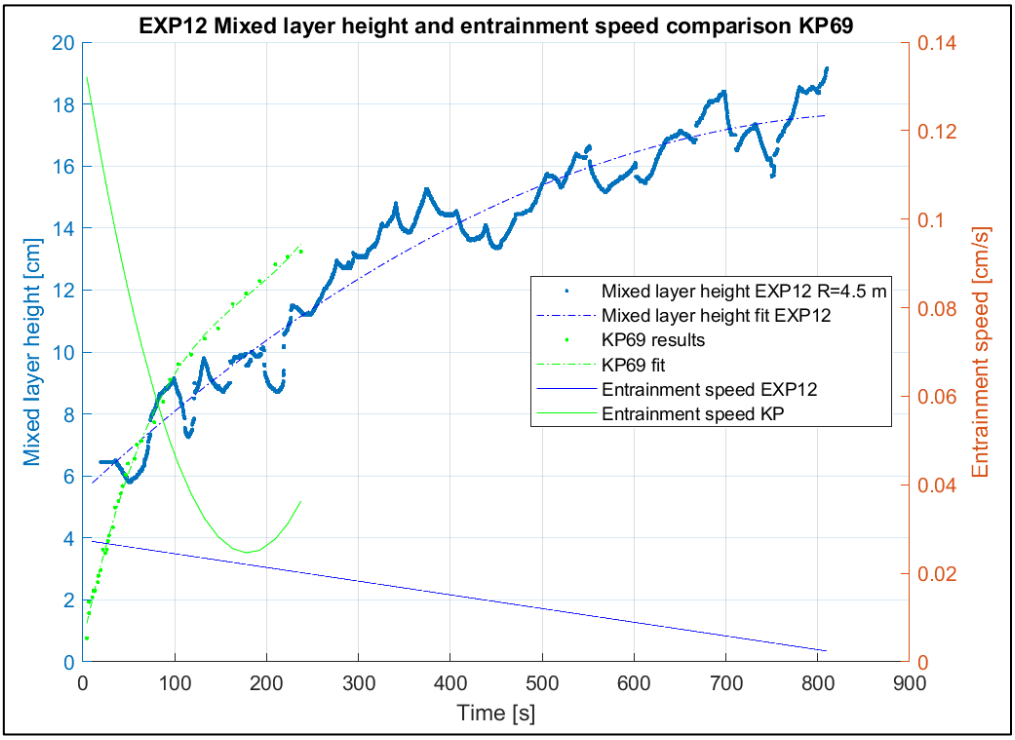

Figure 21: Following KP69 process to estimate the entrainment speed using the mixed layer height

The growth of the mixed layer has been fitted with a parabolic curve and it represents sufficiently well its behaviour.

Dividing by the friction velocity at that radius gives the entrainment coefficient which can be related to the Richardson number:

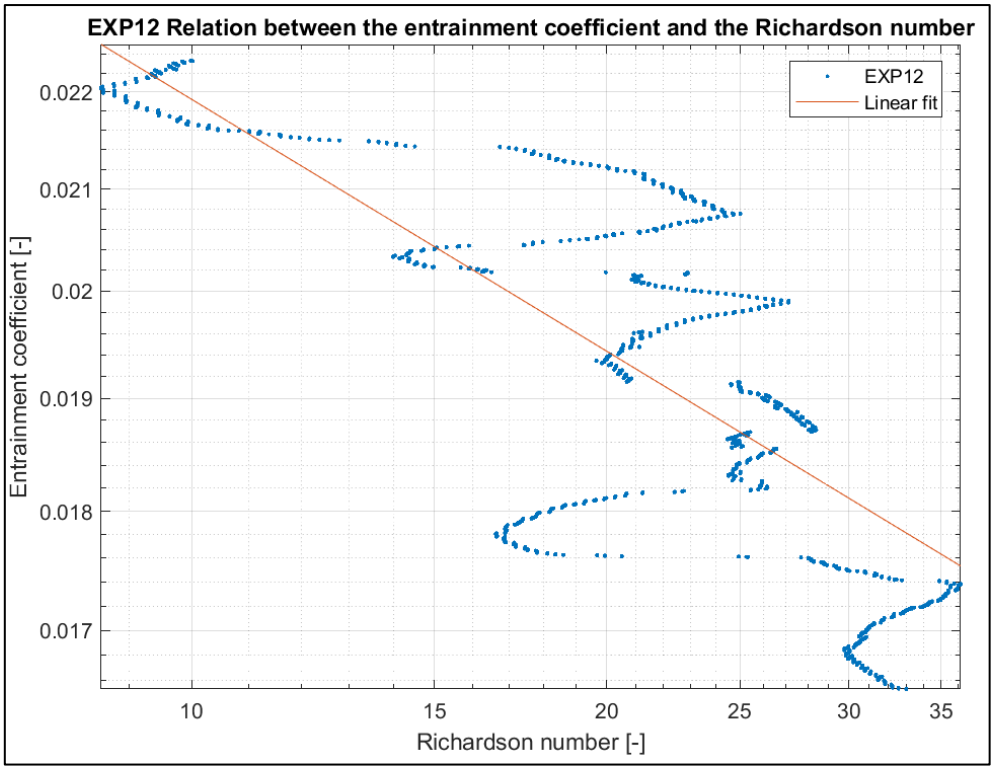

Figure 22: Logarithmic lot of the entrainment coefficient in relation to the Richardson number

Compared to the results of KP69 the relation is of the order of $Ri^{-0.17}$; significantly different than the Ri^{-1} expected; the range of the Richardson number is in the lower values compared to the KP results and this can partly explain the different relation; the bigger uncertainty present is the entrainment speed. From previous analysis of the potential energy, it seems that calculating the entrainment speed from the growth of the mixed layer is not a reliable way to estimate the mixing.

In fact, the values of entrainment speed obtained in EXP12 are significantly weaker than the one obtained by KP69, as can be seen in Figure 21; this seems to hold true only initially, that could be the case because a small homogeneous layer gets formed at the bottom of the tank, even before the start of the spin up in EXP12, so the initial data is not consistent with KP results; but the potential energy measurements show a much more realistic independent relation between mixed layer height and the mixing process overall.

This major difference in entrainment speed justifies the much lower entrainment coefficient compared to the expected relation with the Richardson number.

- The Richardson number is defined as the ratio of the stratification strength and mechanical and inertial effects; a high number means that the stratification is strong and has a major influence over the mechanical effects:

$$Ri = \frac{g}{\rho_0}\frac{d\rho/dz}{(du/dz)^2} = \frac{N^2H^2}{w_h^2} \qquad [15]$$

N^2: Brunt–Väisälä frequency squared [s^{-2}]

H: Characteristic Height [m].

w_h: Characteristic velocity [m/s].

ρ_0: Reference density [kg/m^3].

- The Rayleigh number is defined as the ratio between the buoyancy flux and the viscous and thermal diffusion:

$$Ra = \frac{g\alpha\Delta T H^3}{\nu k} \qquad [16]$$

g: Gravity [m/s^2].

α: Thermal expansion coefficient [K^{-1}].

ΔT: Temperature difference between the hot plate and the water [K].

ν: Kinetic viscosity [m^2/s].

k: Thermal conductivity $\left[\frac{W}{mK}\right]$.

This value was calculated in the second set of experiments in the cases with no temperature stratification over the vertical and no rotation that could influence the heating process:

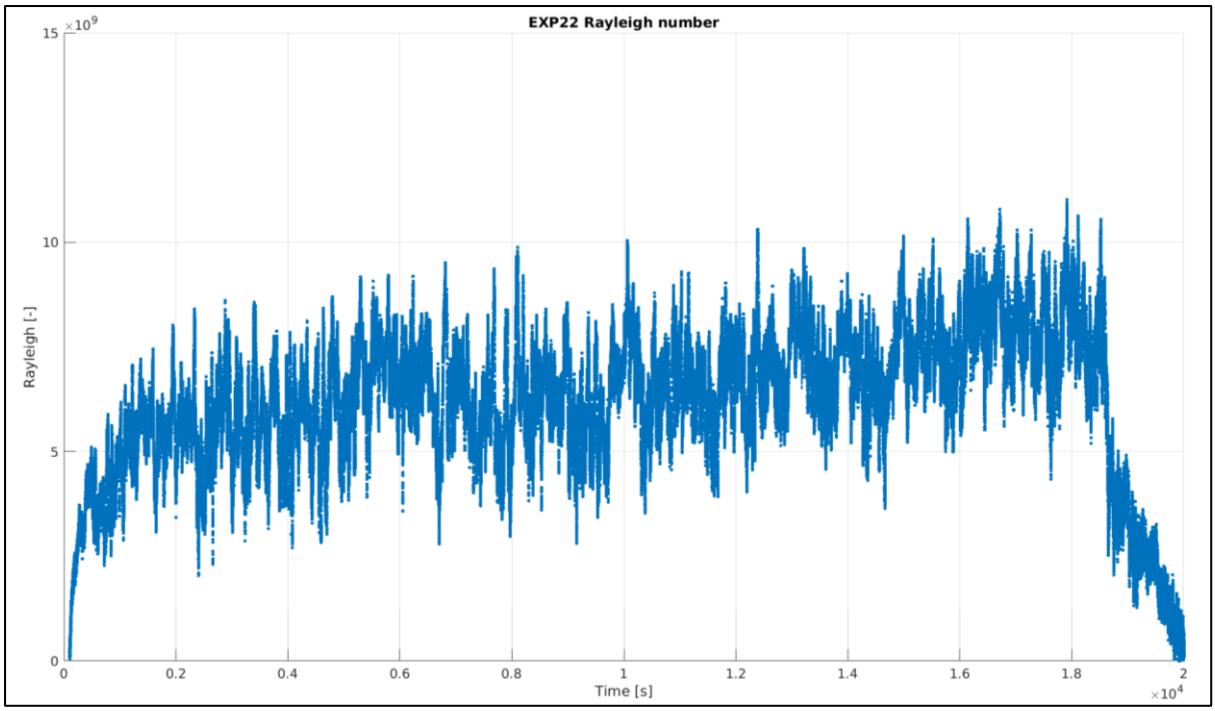

Figure 23: Rayleigh number over time

It can be distinguished easily the moment when the heating plate gets turned on and turned off close to the end of the experiment.

- The Nusselt number is defined as the ratio between the total heat transfer through a boundary to the conductive heat transfer:

$$Nu = \frac{qL}{k\Delta T} \qquad [17]$$

q: Total heat flux through the boundary $\left[\frac{W}{m^2}\right]$.

L: Characteristic vertical length of the experiment [m].

k: Thermal conductivity $\left[\frac{W}{mK}\right]$.

ΔT: Temperature difference between the hot plate and the water [K].

Because the experiment tries to imitate a Rayleigh Benard experiment, in our cases we are using the hypothesis that the actual ΔT and H is double the one in the experiment, this is a strong but realistic hypothesis because the temperature on the homogeneous top layer changes a very small amount over the time of the experiment; in a standard Rayleigh Benard experiment it would remain constant.

The estimations obtained are as follows:

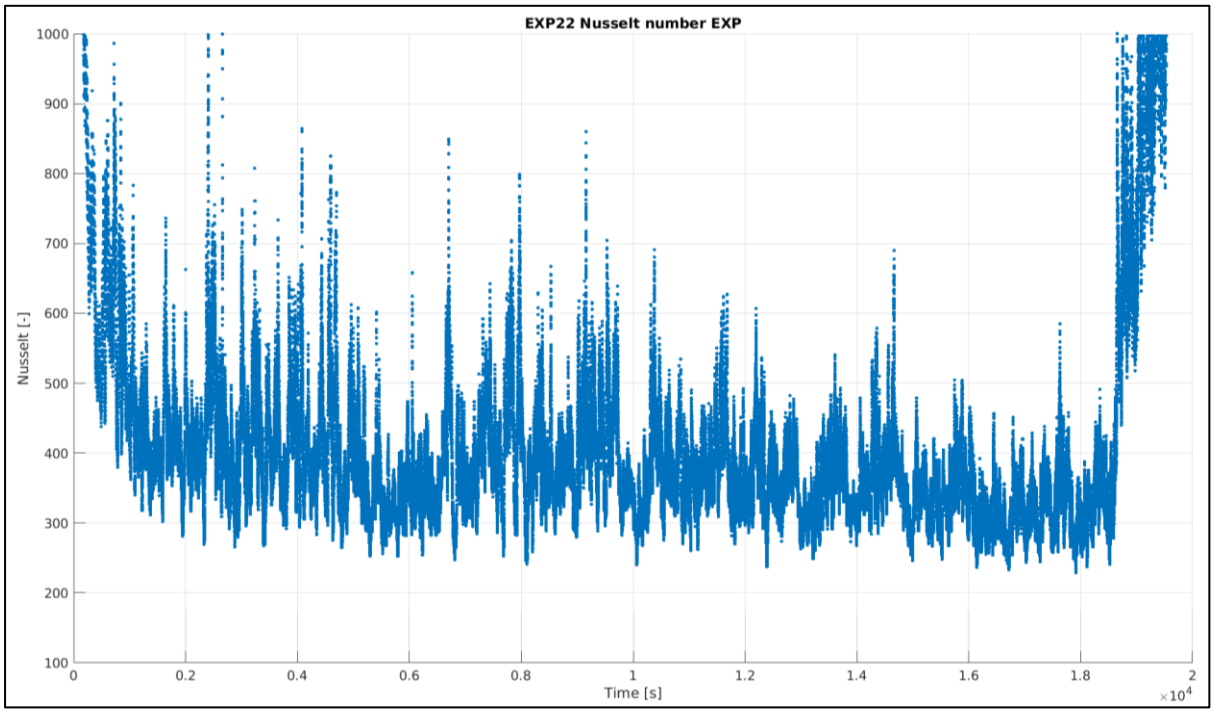

Figure 24: Nusselt number over time

The Nusselt number grows a lot when the plate is turned off because of the ΔT at the denominator.

In both the Rayleigh and the Nusselt number, it's expected that the ΔT used underestimates the real value; the temperature probe has been initially positioned at a

few millimetres from the heating plate, but the thermal layer is very small, the real temperature of the plate could be slightly higher.

In later experiments, the probe has been positioned inside the plate by fitting it in between openings of the metal plates.

- The growth of the mixed layer caused by only heating at the bottom has been studied in the experiments and compared with theoretical results, knowing the heat flux from the plate.

The model starts in a condition where a small homogeneous layer has already been formed such as this:

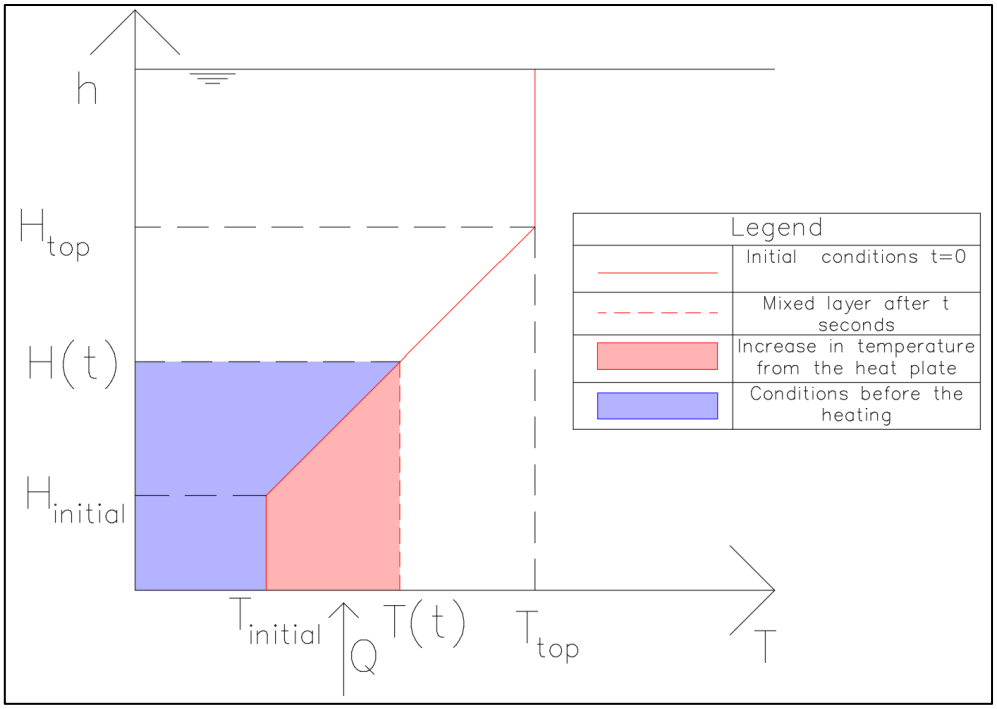

Figure 25: Model used to estimate the theoretical growth of the mixed layer

Knowing the heat flux Q of the plate, this system of equations can easily be created from the above model:

$$\begin{cases} Q\Delta t = c_p\delta\left(T(t)H(t) - T_{in}H_{in} - (H(t) - H_{in})\left(T_{in} + \frac{T(t)-T_{in}}{2}\right)\right) \\ T(t) = T_{in} + \frac{T_{top}-T_{in}}{H_{top}-H_{in}}(H(t) - H_{in}) \end{cases} \quad [18]$$

The first equation defines that all the energy coming from the heating plate goes to the area in red in Figure 25, so, it's equal to the total energy (energy from blue+red areas) minus the energy from the blue areas, which are divided into the two parts visible on the model.

It's not necessary to hypothesize a constant stratification slope; this model can be updated for each time instant changing the slop of the stratification as it evolves over

time; this has been implemented but barely changed the results, in fact, during these experiments, the stratification slope almost never changes as expected.

Solving the system gives the formula to calculate the height of the mixed layer from the starting conditions:

$$H(t) = \left(\sqrt{H_{in}^2 + \frac{2Q}{c_p \rho} \frac{H_{top} - H_{in}}{T_{top} - T_{in}}}\right) \sqrt{\Delta t} \qquad [19]$$

Applying this formula gave these results:

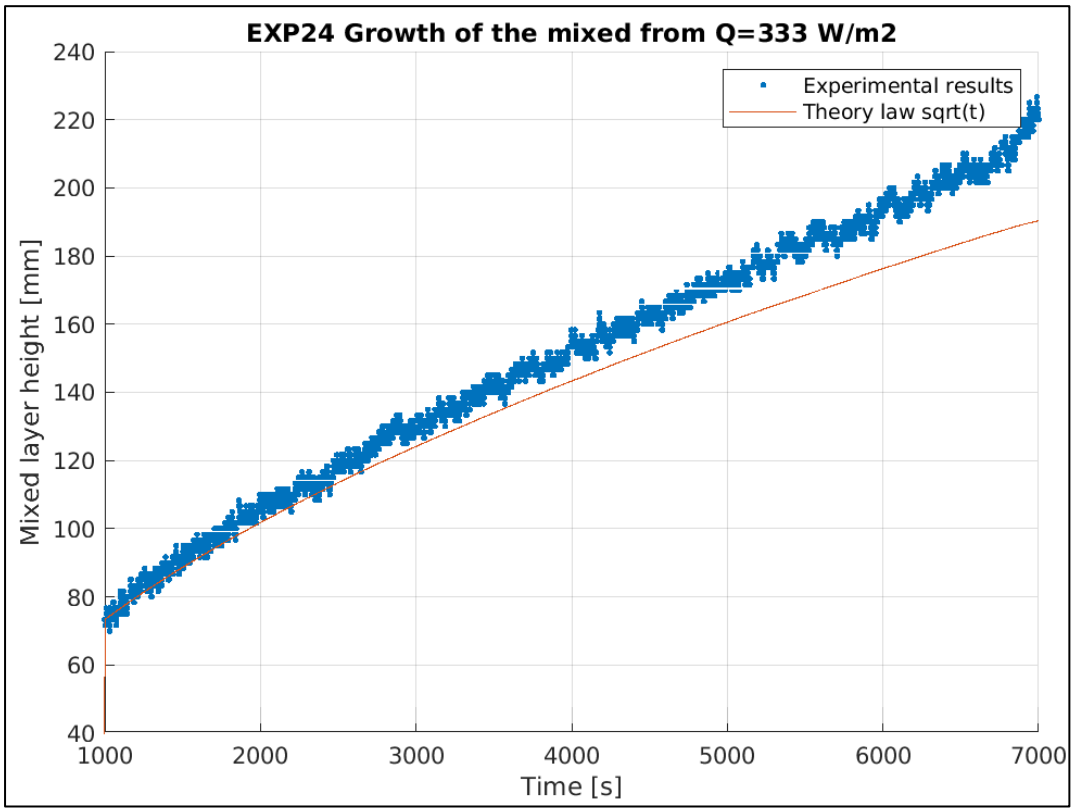

Figure 26: Confronting theory and experimental results growth of the mixed layer

The theoretical solution slightly underestimates the growth of the layer overall, but this can be explained by the fact that the plumes moving inside the tank caused partial mixing which can increase the growth of the mixed layer. The fitting was only expected to work well for short amount of times before other smaller phenomena started taking effect on the mixed layer height.

The heat flux assumed is 333 W/m^2 which is consistent with the previous calculations regarding the heat flux.

Conclusions

During my stage period at the LEGI, I learned to study and analyse lots of data and obtained various interesting results; the phenomenon studied is very complex and it's hard to find many detailed studies on scientific journals, this made very difficult comparing results with the state of the art with my current knowledge and time constraints.

Regardless of this, a lot of interesting data has been obtained and some interesting conclusions have been obtained, such as:

- The independence between the growth of the mixed layer and the mixing process overall after the analysis regarding the potential energy change over time in the first set of experiments.
- The comparison between P73 and experimental results of the growth of the mixed layer in a rotating ambient, which showed good similarity between them even considering the different approach used in regard of the Brunt–Väisälä frequency which cannot be considered constant in the first set of experiments done.
- The good similarity between the experimental and theoretical growth of the mixed layer in the second set of experiments with only the heating from the bottom plate applied.
- The qualitative progression of the temperature profiles over time which is consistent with expectations both in the first and second set of experiments.

The codes that I've developed have all been shared with the research team and made as easy as possible to read and use, for any doubt regarding them I remain available for questions and further contacts in case it becomes necessary.

I want to thank all researchers and members of the LEGI team that have helped and supported me during the stage significantly, both from a technical and theoretical point of view:

- Referent researchers: Maria Eletta Negretti, Joel Sommeria
- PhD students: Max Coppin, Antonio Ammendola
- Engineers working at the Coriolis Platform: Samuel Viboud, Thomas Valran

Bibliography

Koenigk, T., Fuentes-Franco, R., Meccia, V.L. *et al* (2021). *"Deep mixed ocean volume in the Labrador Sea in HighResMIP models"*. *Clim Dyn* **57**, 1895–1918.

Huang, C. J., F. Qiao, and D. Dai (2014). "Evaluating CMIP5 simulations of mixed layer depth during summer". *J. Geophys. Res. Oceans*, 119, 2568–2582.

Kato H, Phillips OM (1969). "On the penetration of a turbulent layer into stratified fluid". *Journal of Fluid Mechanics*.

POLLARD, Raymond T.; RHINES, Peter B.; THOMPSON, Rory ORY. The deepening of the wind-mixed layer. _Geophysical Fluid Dynamics_, 1973, 4.4: 381-404.

TURNER, J. S. The influence of molecular diffusivity on turbulent entrainment across a density interface. _Journal of Fluid Mechanics_, 1968, 33.4: 639-656.

George S. Kell (1975). "Density, thermal expansivity, and compressibility of liquid water from 0.deg. to 150.deg.. Correlations and tables for atmospheric pressure and saturation reviewed and expressed on 1968 temperature scale". *Journal of Chemical & Engineering Data* **1975** *20* (1), 97-105

Sous, D. et al. (2013). "Friction law and turbulent properties in a laboratory Ekman boundary layer". Phys. Fluids, pp. 046602-046602–18.